Journal of the Ceramic Society of Japan 117 [1] 37-41 2009 **Paper**

Syntheses and crystal structures of Si-bearing layered carbides $ZrAl_8C_7$ and $ZrAl_4C_4$

Tomoyuki IWATA, Eriko HATTORI, Keita SUGIURA, Shinobu HASHIMOTO, Hiromi NAKANO* and Koichiro FUKUDA†

Department of Environmental and Materials Engineering, Nagoya Institute of Technology, Gokiso-cho, Showa-ku, Nagoya 466−8555
***Electron Microscope Laboratory, Ryukoku University, Yokotani, Seta Oe-cho, Otsu 520−2194**

Two types of new quaternary carbide solid solutions, $(ZrC)[Al_{1-x}Si_x]_8C_6$ with $x = 0.06$ and $(ZrC)[Al_{1-y}Si_y]_4C_3$ with $y = 0.04$, have been synthesized and characterized using a laboratory X-ray powder diffraction (Cu Kα_1), transmission electron microscopy and energy dispersive X-ray spectroscopy (EDX). The average atom ratios [Al:Si] of both carbides were determined by EDX, and the crystal structures were refined using the Rietveld method. These carbides have been found to form a homologous series with the general formula $(ZrC)_m[Al_{1-z}Si_z]_8C_6$ ($0 \le z \le 0.07$), where $m = 1$ and 2. The crystal structures can be regarded as intergrowth structures, consisting of the NaCl-type $[Zr_mC_{m+1}]$ slabs separated by the Al_4C_3-type $[(Al_{1-z}Si_z)_8C_7]$ layers.

Key-words : Layered carbides, Solid solutions, Crystal structures, Powder diffraction, Rietveld refinement

[Received August 6, 2008; Accepted September 11, 2008]

1. Introduction

In the system Zr–Al–C, two types of new ternary carbides, $(ZrC)Al_8C_6$[1] and $(ZrC)Al_4C_3$,[2] have been synthesized at 2273 K and structurally characterized by X-ray powder diffraction (XRPD) method. These carbides form a homologous series with the general formula $(ZrC)_mAl_8C_6$ ($m = 1$ and 2).[1] Both crystal structures, although belonging to the different space groups $R\bar{3}m$ for $m = 1$ and $P3m1$ for $m = 2$, can be regarded as intergrowth structures where the Al_4C_3-type $[Al_8C_7]$ layers are the same, while the NaCl-type $[Zr_mC_{m+1}]$ layers increase in thickness with increasing m value. In the ternary system, the other carbides reported so far are $(ZrC)_2Al_4C_3$, $(ZrC)_3Al_4C_3$, $(ZrC)_2Al_3C_2$ and $(ZrC)_3Al_3C_2$.[3)–5)] The former two carbides, which have been synthesized at 2073 K, also form a homologous series with the general formula of $(ZrC)_mAl_4C_3$ ($m = 2$ and 3).[3] The considerable amounts of Si component have been found to dissolve into the $[Al_4C_4]$ layers of $(ZrC)_mAl_4C_3$ at the lower temperatures than 2073 K (*i.e.*, 1873–1973 K) to stabilize the crystal structures.[3),6),7)] Thus, the ternary carbides $(ZrC)_mAl_4C_3$ are considered to be the end members of the solid solutions. Because the atomic scattering factors for Al and Si are almost the same, these atoms were assumed to be randomly distributed over the same sites in the Al_4C_3-type layers, although there might be the site preference of these atoms.

Thermoelectric materials with high efficiency of energy conversion are of interest for applications as heat pumps and power generators. Low-dimensional materials that consist of, for example, conducting two-dimensional (2D) layers are promising for thermoelectric energy conversion.[8)–11)] The advantage of the low dimensionality can be interpreted in terms of the carrier confinement effect in the 2D layers, which leads to an enlarged absolute value of the Seebeck coefficient compared to the materials with three-dimensional conducting paths. The crystal structures of the layered carbides in the Zr–Al–C and/or Zr–Al–Si–C systems are composed of the electroconductive $[Zr_mC_{m+1}]$ layers separated by the less conductive [(Al,Si)C] layers. Hence, the homologous carbides demonstrated good performance of thermoelectricity, and regarded as the promising thermoelectric materials.[6),7)]

In the present study, we have successfully dissolved the Si component into the $[Al_8C_7]$ layers of $(ZrC)_mAl_8C_6$ ($m = 1$ and 2) to stabilize the crystal structures at 2073 K, which is 200 K lower than the formation temperature of the end members.

2. Experimental procedure

2.1 Materials

In the reacted ZrC–Al_4C_3–SiC mixtures, two types of new quaternary carbides were initially recognized by their very similar diffraction patterns to those of $(ZrC)_mAl_8C_6$ with $m = 1$ and 2.[1),2)] Since the present specimens contain Si component, the new carbides are most probably of Si-dissolved $(ZrC)_mAl_8C_6$ solid solutions. We obtained, by the following procedures, the two types of powder samples; one consisted mainly of (ZrC)[Al, Si]$_8C_6$ (sample S-A) and the other was mainly composed of (ZrC)[Al,Si]$_4C_3$ (S-B).

The reagent-grade chemicals of ZrC (99.9%, KCL Co., Ltd., Saitama, Japan), Al_4C_3 (KCL, 99.9%) and SiC (KCL, 99.9%) were mixed in two different molar ratios of [ZrC:Al_4C_3:SiC] = [1:3:1] for S-A and [4:6:1] for S-B. Each of the well-mixed chemicals was pressed into pellets (ϕ 13 mm × 10 mm), heated at 2073 K for 1 h in vacuum, followed by cooling to ambient temperature by cutting furnace power. Both reaction products were slightly sintered polycrystalline materials. They were finely ground to obtain powder specimens. Small amounts of Al_4C_3 crystallites coexisted in both samples. These crystals in S-B were completely removed by dissolution with acid solution. On the other hand, the crystals of (ZrC)[Al,Si]$_8C_6$ also dissolved in the acid solution. Hence, the acid treatment of selectively dissolving the Al_4C_3 compound was inapplicable to the sample S-A.

† Corresponding author: K. Fukuda; E-mail: fukuda.koichiro@nitech.ac.jp

2.2 Characterization

XRPD intensities were collected on a diffractometer (X'Pert PRO Alpha-1, PANalytical B.V., Almelo, The Netherlands) equipped with a high speed detector in Bragg–Brentano geometry using monochromatized Cu Kα_1 radiation (45 kV, 40 mA) in a 2θ range from 2.0052° to 148.9056° (an accuracy in 2θ of ± 0.0001°). The divergence slit of 0.25° and the automatic divergence slit were employed, respectively, for samples S-A and S-B to collect the quantitative profile intensities over the whole 2θ range. Other experimental conditions were: continuous scan, total of 17582 datapoints and total experimental time of 5.0 h. The crystal-structure models were visualized with the computer program VESTA.[12)]

The powder specimens were examined using transmission electron microscopes (JEM 3000F and JEM 2010, JEOL Ltd., Tokyo, Japan) and equipped with an energy dispersive X-ray analyzer (EDX; VOYAGER III, NORAN Instruments, Middleton, WI, USA). The powder particles were deposited with ethyl alcohol on a copper grid. Selected area electron diffraction (SAED) patterns and corresponding lattice images were obtained. Chemical analyses were made for eight crystal frag-

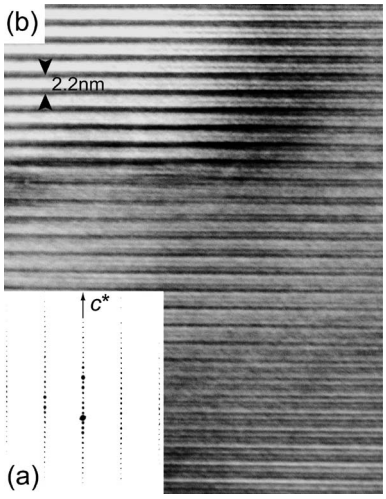

Fig. 1. (a) Selected-area electron diffraction pattern and (b) corresponding lattice fringe image showing periodicity of about 2.2 nm (= c). Incident beam perpendicular to the c-axis. Sample $(ZrC)[Al_{0.96}Si_{0.04}]_4C_3$ in S-B.

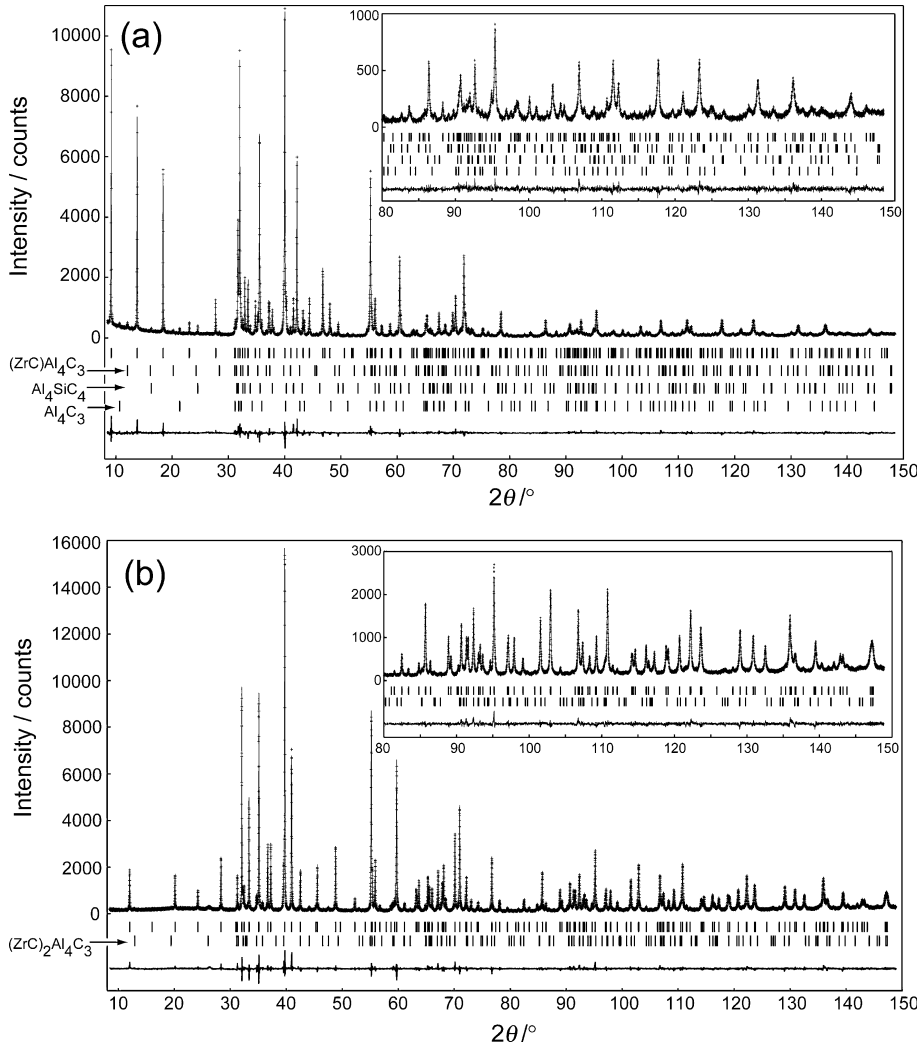

Fig. 2. Comparison of the observed diffraction patterns (symbol: +) with the corresponding calculated patterns (upper solid lines). The difference curves are shown in the lower part of the diagrams. Upper vertical bars in each diagram indicate the positions of possible Bragg reflections. The profile intensities for (a) $(ZrC)[Al_{0.94}Si_{0.06}]_8C_6$, $(ZrC)Al_4C_3$, Al_4SiC_4 and Al_4C_3 in S-A and (b) $(ZrC)[Al_{0.96}Si_{0.04}]_4C_3$ and $(ZrC)_2Al_4C_3$ in S-B.

ments of (ZrC)[Al, Si]$_8$C$_6$ in S-A and seven fragments of (ZrC)[Al,Si]$_4$C$_3$ in S-B to determine the individual atom ratios [Al:Si]. The corrections were made by the ZAF routines.

3. Results and discussion

3.1 Structure refinement

The SAED pattern [**Fig. 1**(a)] of (ZrC)[Al,Si]$_4$C$_3$ in S-B was successfully indexed with a hexagonal unit cell with dimensions of $a \approx 0.33$ nm and $c \approx 2.2$ nm. The corresponding lattice image [Fig. 1(b)] strongly suggests that the crystal structure is built up from stacking combinations of two basic sheets. The presence of Si atoms within both carbides has been well confirmed by the EDX analysis. In S-A, the average atom ratios [Zr:Al:Si] were found to be [10.9(1.3):83.9(1.8):5.3(1.2)], where the figures in parentheses indicate standard deviations. The atom ratios are almost equivalent to [Zr:Al+Si] = [1:8], with the [Al:Si] ratios being [0.94(1):0.06(1)] on the basis of Al + Si = 1. The [Al:Si] ratios of the carbide in S-B were determined to be [0.96(1):0.04(1)] based on the average atom ratios of [Zr:Al:Si] = [20.2(1.5):76.7(2.2):3.1(0.8)], which are nearly equivalent to [Zr:Al + Si] = [1:4]. Accordingly, the chemical formulas would be satisfactorily represented by (ZrC)[Al$_{0.94(1)}$Si$_{0.06(1)}$]$_8$C$_6$ in S-A and (ZrC)[Al$_{0.96(1)}$Si$_{0.04(1)}$]$_4$C$_3$ in S-B.

Initial structural parameters of (ZrC)[Al$_{0.94}$Si$_{0.06}$]$_8$C$_6$ and (ZrC)[Al$_{0.96}$Si$_{0.04}$]$_4$C$_3$ were taken from those determined by Iwata et al. for (ZrC)Al$_8$C$_6$ and (ZrC)Al$_4$C$_3$, respectively.[1),2)] The structural parameters were individually refined by the Rietveld method using the computer program RIETAN-FP.[13)] The structure models of Al$_4$C$_3$,[14)] Al$_4$SiC$_4$,[15)] (ZrC)Al$_4$C$_3$[2)] and (ZrC)$_2$Al$_4$C$_3$[3)] were added into the refinement as additional phases. A Legendre polynomial was fitted to background intensities with twelve adjustable parameters. The split Pearson VII function[16)] was used to fit the peak profile. The Al and Si atoms were assumed to be randomly distributed over the same sites (denoted by T sites) in the crystal structures without any constrains onoccupancies, although there might be the site preference of these atoms. All of the isotropic atomic displacement parameters (B) of carbon atoms were constrained to have the same value. The reliability indices[17)] for the final result of S-A were R_{wp} = 8.03%, S = 1.24 and R_p = 6.01% (R_B = 2.33% and R_F = 1.18% for (ZrC)[Al$_{0.94}$Si$_{0.06}$]$_8$C$_6$) [**Fig. 2**(a)] and those of S-B were R_{wp} = 6.93%, S = 1.30 and R_p = 5.31% (R_B = 1.94% and R_F = 1.07% for (ZrC)[Al$_{0.96}$Si$_{0.04}$]$_4$C$_3$) [Fig. 2(b)]. Crystal data are given in **Tables 1** and **2**, and the final atomic positional and B parameters are given in **Tables 3** and **4**. Quantitative X-ray analysis with correction for microabsorption according to Brindley's procedure[18)] was implemented in the program RIETAN-FP. The phase compositions were determined to be 76.4 mass% (ZrC)[Al$_{0.94}$Si$_{0.06}$]$_8$C$_6$, 13.1 mass% Al$_4$SiC$_4$, 5.4 mass% Al$_4$C$_3$ and 5.1 mass% (ZrC)Al$_4$C$_3$ for S-A and 92.6 mass% (ZrC)[Al$_{0.96}$Si$_{0.04}$]$_4$C$_3$ and 7.4 mass% (ZrC)$_2$Al$_4$C$_3$ for S-B.

Table 1. Crystal Data for (ZrC)[Al$_{0.94}$Si$_{0.06}$]$_8$C$_6$

Chemical composition	ZrAl$_{7.52}$Si$_{0.48}$C$_7$
Space group	R$\bar{3}m$
a/nm	0.332214 (3)
c/nm	5.78236 (5)
V/nm^3	0.552678(8)
Z	3
D_x/Mgm^{-3}	3.53

Table 2. Crystal Data for (ZrC)[Al$_{0.96}$Si$_{0.04}$]$_4$C$_3$

Chemical composition	ZrAl$_{3.84}$Si$_{0.16}$C$_4$
Space group	$P3m1$
a/nm	0.332349 (1)
c/nm	2.199241 (7)
V/nm^3	0.210375 (1)
Z	2
D_x/Mgm^{-3}	3.91

Table 3. Structural Parameters for (ZrC)[Al$_{0.94}$Si$_{0.06}$]$_8$C$_6$

Site	Wyckoff position	x	y	z	$100 \times B$/nm^2
Zr	3b	0	0	1/2	0.63(3)
T1	6c	0	0	0.05647(3)	0.46(4)
T2	6c	0	0	0.12772(4)	0.41(3)
T3	6c	0	0	0.24448(3)	0.54(4)
T4	6c	0	0	0.31628(3)	0.50(5)
C1*	3a	0	0	0	0.50(6)
C2	6c	0	0	0.0933(1)	0.50
C3	6c	0	0	0.19092(9)	0.50
C4	6c	0	0	0.28286(9)	0.50

*z of C1 atom is fixed.

Table 4. Structural Parameters for (ZrC)[Al$_{0.96}$Si$_{0.04}$]$_4$C$_3$

Site	Wyckoff position	x	y	z	$100 \times B$/nm^2
Zr1	1c	2/3	1/3	0.6824(9)	0.61(6)
Zr2	1b	1/3	2/3	0.8031(9)	0.61(6)
T1	1c	2/3	1/3	0.0122(10)	0.9(1)
T2	1c	2/3	1/3	0.1976(12)	0.9(3)
T3	1b	1/3	2/3	0.2889(12)	0.6(3)
T4	1b	1/3	2/3	0.4829(10)	1.0(1)
T5	1a	0	0	0.0930(11)	0.9(3)
T6	1a	0	0	0.3938(11)	0.8(3)
T7	1a	0	0	0.5812(10)	0.7(2)
T8	1a	0	0	0.9089(11)	0.7(2)
C1	1c	2/3	1/3	0.1069(12)	0.67(7)
C2	1c	2/3	1/3	0.8754(10)	0.67
C3	1b	1/3	2/3	0.3729(13)	0.67
C4	1b	1/3	2/3	0.6223(9)	0.67
C5*	1a	0	0	0	0.67
C6	1a	0	0	0.2458(15)	0.67
C7	1a	0	0	0.4911(4)	0.67
C8	1a	0	0	0.7404(16)	0.67

*z of C5 atom is fixed.

The EDX analysis showed that the atom ratios of both quaternary carbides varied slightly but certainly from crystal fragment to fragment, indicating that these carbides are not compounds but solid solutions. The atom ratios [Al:Si] in S-A almost varied from [0.95:0.05] to [0.93:0.07], indicating that the maximum Si/(Al + Si)-value is most probably 0.07. Thus, the carbide solid solution would be satisfactorily represented by the general formula $(ZrC)[Al_{1-x}Si_x]_8C_6$ with $0 \le x \le 0.07$. In the same manner, the chemical variation in S-B was within the solid-solution range of $0 \le y \le 0.05$ for $(ZrC)[Al_{1-y}Si_y]_4C_3$, because the [Al:Si] ratios almost ranged from [0.97:0.03] to [0.95:0.05].

3.2 Structure description

The crystal structures may be regarded as intergrowth structures (**Fig. 3**), which consist of the NaCl-type $[Zr_mC_{m+1}]$ layers (thickness of ~0.28 nm for $m = 1$ and ~0.56 nm for $m = 2$) separated by the Al_4C_3-type $[(Al_{1-z}Si_z)_8C_7]$ layers with ~1.64 nm thickness ($0 \le z \le 0.07$). The selected interatomic distances,

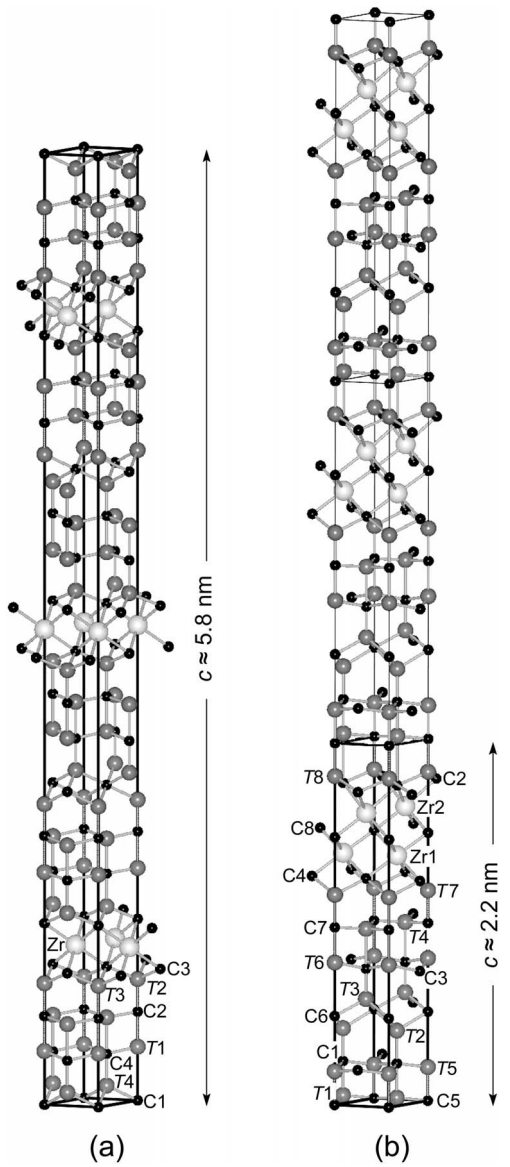

Fig. 3. Crystal structures of $(ZrC)[Al_{0.94}Si_{0.06}]_8C_6$ in (a) and $(ZrC)[Al_{0.96}Si_{0.04}]_4C_3$ in (b). The Al and Si atoms are assumed to be randomly distributed on the *T* sites for both crystal structures.

Table 5. Interatomic Distances (nm) in $(ZrC)[Al_{0.94}Si_{0.06}]_8C_6$*

Zr–C3	0.2376(3) × 6
Zr–*T*2	0.2959(2) × 6
*T*1–C4	0.1949(1) × 3
*T*1–C2	0.2127(6)
*T*1–*T*3	0.2681(2) × 3
*T*1–*T*4	0.2979(2) × 3
*T*2–C2	0.1992(6)
*T*2–C3	0.2098(2) × 3
*T*2–*T*3	0.2954(2) × 3
*T*3–C2	0.19349(8) × 3
*T*3–C4	0.2219(5)
*T*4–C4	0.1933(5)
*T*4–C1	0.21566(9) × 3
*T*4–*T*4	0.2751(3) × 3

*All distances shorter than 0.30 nm (metal–metal) and 0.24 nm (metal–carbon) are given.

Table 6. Interatomic Distances (nm) in $(ZrC)[Al_{0.96}Si_{0.04}]_4C_3$*

Zr1–C8	0.230(1) × 3
Zr1–C4	0.2331(7) × 3
Zr1–*T*7	0.294(1) × 3
Zr2–C8	0.236(2) × 3
Zr2–C2	0.249(1) × 3
Zr2–*T*8	0.3016(9) × 3
*T*1–C5	0.1937(3) × 3
*T*1–C1	0.208(1)
*T*1–*T*5	0.2616(9) × 3
*T*1–*T*8	0.2974(9) × 3
*T*2–C1	0.199(2)
*T*2–C6	0.219(1) × 3
*T*2–*T*3	0.2778(2) × 3
*T*2–*T*5	0.299(1) × 3
*T*3–C3	0.185(2)
*T*3–C6	0.214(1) × 3
*T*3–*T*6	0.300(1) × 3
*T*4–C7	0.1927(2) × 3
*T*4–C3	0.242(2)
*T*4–*T*6	0.274(1) × 3
*T*4–*T*7	0.289(1) × 3
*T*5–C1	0.1943(3) × 3
*T*5–C5	0.205(2)
*T*6–C3	0.1973(4) × 3
*T*6–C7	0.214(2)
*T*7–C7	0.198(2)
*T*7–C4	0.2121(7) × 3
*T*8–C5	0.200(2)
*T*8–C2	0.2055(8) × 3

*All distances shorter than 0.31 nm (metal–metal) and 0.25 nm (metal–carbon) are given.

together with their standard deviations, are given in **Tables 5** and **6**. The mean interatomic distances in $(ZrC)[Al_{0.94}Si_{0.06}]_8C_6$ and $(ZrC)[Al_{0.96}Si_{0.04}]_4C_3$ compare well with those of ZrC, Al_4C_3, $(ZrC)Al_8C_6$ and $(ZrC)Al_4C_3$. The Zr sites are octahedrally coordinated by C atoms with the mean distances of 0.238 nm for m = 1 and 0.237 nm for m = 2, which are comparable to those of the ZrC_8 polyhedra in ZrC (0.235 nm), $(ZrC)Al_8C_6$ (0.238 nm) and $(ZrC)Al_4C_3$ (0.237 nm).[1),4),5)] The mean Zr–T distances of 0.296 nm for m = 1 and 0.298 nm for m = 2 are comparable to the Zr–Al distances of $(ZrC)Al_8C_6$ (0.298 nm) and $(ZrC)Al_4C_3$ (0.299 nm). The T sites are tetrahedrally coordinated with the mean distances of 0.204 nm for both m = 1 and m = 2. These T–C distances are comparable to the Al–C distances of the AlC_4 tetrahedra in Al_4C_3 ranging from 0.194 to 0.218 nm (the mean = 0.206 nm),[10)] which implies that the $[(Al_{1-z}Si_z)_8C_7]$ layers of both m = 1 and m = 2 are structurally comparable to the compound Al_4C_3. Accordingly, these carbide solid solutions form a homologous series with the general formula of $(ZrC)_m[Al_{1-z}Si_z]_8C_6$ (m = 1 and 2) with $0 \le z \le 0.07$.

4. Conclusions

In the Zr–Al–Si–C system, we have successfully synthesized the two types of new carbide solid solutions $(ZrC)[Al_{1-x}Si_x]_8C_6$ (x = 0.06) and $(ZrC)[Al_{1-y}Si_y]_4C_3$ (y = 0.04), the end members of which were, respectively, $(ZrC)Al_8C_6$ and $(ZrC)Al_4C_3$. The crystal structures were considered to be composed of the NaCl-type $[Zr_mC_{m+1}]$ slabs separated by the Al_4C_3-type $[(Al_{1-z}Si_z)_8C_7]$ layers, and hence they formed a homologous series with the general formula of $(ZrC)_m[Al_{1-z}Si_z]_8C_6$ (m = 1 and 2) with $0 \le z \le 0.07$.

Acknowledgments Supported by a Grant-in-Aid for Scientific Research (No. 18560654) from the Japan Society for the Promotion of Science, and a grant from the Research Foundation for the Electrotechnology of Cubu.

References

1) T. Iwata, K. Sugiura, S. Hashimoto and K. Fukuda, *J. Am. Ceram. Soc.*, in press.
2) T. Iwata, E. Hattori, S. Hashimoto and K. Fukuda, *J. Am. Ceram. Soc.*, in press.
3) K. Sugiura, T. Iwata, H. Yoshida, S. Hashimoto and K. Fukuda, *J. Solid State Chem.*, 181, 2864–2868 (2008).
4) K. Fukuda, S. Mori and S. Hashimoto, *J. Am. Ceram. Soc.*, 88, 3528–3530 (2005).
5) Th. M. Gesing and W. Jeitschko, *J. Solid State Chem.*, 140, 396–401 (1998).
6) K. Fukuda, M. Hisamura, T. Iwata, N. Tera and K. Sato, *J. Solid State Chem.*, 180, 1809–1815 (2007).
7) K. Fukuda, M. Hisamura, Y. Kawamoto and T. Iwata, *J. Mater. Res.*, 22, 2888–2894 (2007).
8) L. D. Hicks and M. S. Dresselhaus, *Phys. Rev.*, B47, 12727–12731 (1993).
9) L. D. Hicks and M. S. Dresselhaus, *Phys. Rev.*, B47, 16631–16634 (1993).
10) L. D. Hicks, T. C. Harman and M. S. Dresselhaus, *Appl. Phys. Lett.*, 63, 3230–3232 (1993).
11) K. Koumoto, H. Koduka and W.-S. Seo, *J. Mater. Chem.*, 11, 251–252 (2001).
12) F. Izumi and K. Momma, *Solid State Phenom.*, 130, 15–20 (2007).
13) F. Izumi and T. Ikeda, *Mater. Sci. Forum*, 321–324, 198–203 (2000).
14) Th. M. Gesing and W. Jeitschko, *Z. Naturforsch.*, 50b, 196–200 (1995).
15) Z. Inoue, Y. Inomata, H. Tanaka and H. Kawabata, *J. Mat. Sci.*, 15, 575–580 (1980).
16) H. Toraya, *J. Appl. Crystallogr.*, 23, 485–491 (1990).
17) R. A. Young, "The Rietveld Method," Ed. by R. A. Young, Oxford University Press, Oxford, U.K. (1993) pp. 1–38.
18) G. W. Brindley, *Bulletin de la Societe Chimique de France*, D59–D63 (1949).